

## DETECTION OF PHOSPHOROUS IN INDUSTRIAL OXIDE MATERIALS BY LASER-INDUCED BREAKDOWN SPECTROSCOPY IN THE UV SPECTRAL RANGE\*

E. LJUTIC<sup>1</sup>, P. KOLMHOFFER<sup>1</sup>, H. HEILBRUNNER<sup>1</sup>, B. PRAHER<sup>1</sup>, N. HUBER<sup>1</sup>, R. RÖSSLER<sup>2</sup>,  
H. WOLFMEIR<sup>2</sup>, E. ARENHOLZ<sup>2</sup>, J. HEITZ<sup>1</sup>, J.D. PEDARNIG<sup>1</sup>

<sup>1</sup> Institute of Applied Physics, “Christian Doppler” Laboratory for Laser-Assisted Diagnostics,  
Johannes Kepler University Linz, A-4040 Linz, Austria

E-mail: johannes.heizt@jku.at; johannes.pedarnig@jku.at

<sup>2</sup> voestalpine Stahl GmbH, A-4031 Linz, Austria

Received October 22, 2013

*Abstract.* Detection of phosphorous in optical emission spectroscopy is performed usually below 180 nm with evacuated or purged optical beam paths. However, many applications of laser-induced breakdown spectroscopy (LIBS) require detection in air. We report on LIBS analysis of phosphorous in industrial oxide materials in air using the UV emission line at 214.915 nm.

*Key words:* laser-induced plasma, laser-induced breakdown spectroscopy, element analysis, complex oxides.

### 1. INTRODUCTION

The basis of optical emission spectroscopy (OES) analysis of materials is the fact that in a plasma, the light emitted by excited atoms and ions is unique for each chemical element. The characteristic emission spectra can be used to identify and quantify the elements of which a substance consists. There exist several possible plasma excitation methods. The most common ones are the electrode spark and the inductively coupled plasma (ICP). With the development of the laser in the 1960s a new plasma source became available. In laser-induced breakdown spectroscopy (LIBS) intense laser pulses are used for material ablation and excitation [1–3]. A scheme of a typical LIBS set-up is shown in Fig. 1.

\* Paper presented at the 16<sup>th</sup> International Conference on Plasma Physics and Applications, June 20–25, 2013, Magurele, Bucharest, Romania.

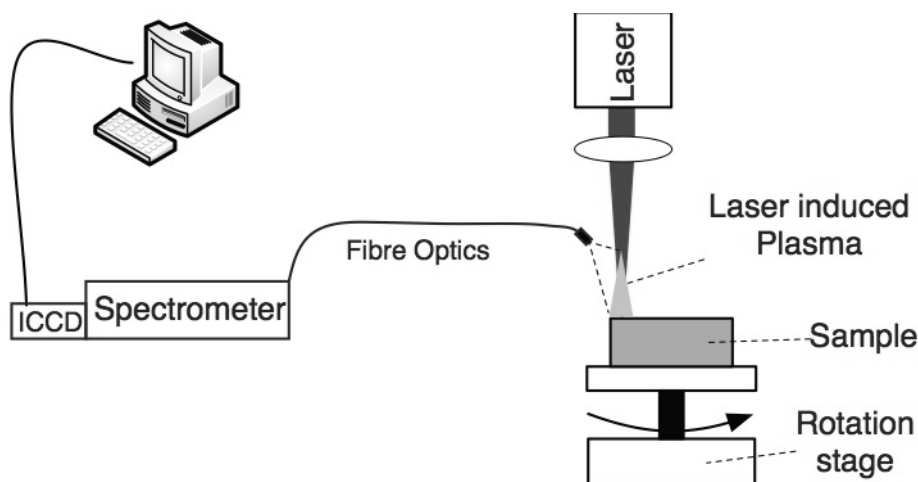


Fig. 1 – Schematic of experimental setup for laser-induced breakdown spectroscopy.

The use of laser pulses for material ablation and plasma ignition in LIBS has many advantages in comparison to conventional techniques. The ability to perform LIBS measurements in-line, remotely and fast can allow monitoring of industrial processes and the analysis of materials in hazardous or otherwise harsh conditions. The material to be analyzed can be solid, liquid or gaseous, conducting or non-conducting, and a pre-treatment is not necessary. Another advantage of LIBS is that only a very small amount of material is required for measurements, which makes it almost non-destructive.

The detection of phosphorous in OES is performed usually in the vacuum ultraviolet spectral range, as the most intense emission lines of (neutral) P I are at wavelengths below 180 nm and as these lines are not spectrally overlapped with other emission lines of typical matrix elements (*e.g.*, Fe, Ca, Al, ...). Measurements in this range require however evacuated or purged optical beam paths to avoid absorption of radiation by oxygen and water vapor in air. Many applications of LIBS, on the other hand, require detection in air at atmospheric pressure, *e.g.*, for on-site measurements in industrial processes.

We report on the detection and quantification of phosphorous in industrial oxide materials by LIBS in air or under argon flow using the UV emission P I line at 214.915 nm. This line is indicated in Fig. 2 together with a neighboring P I line, which is a doublet. The materials studied include iron oxide ceramics, slag from industrial steel production, and certified reference materials. We compare the measured LIBS signals for P with data from reference analysis and tentatively correlate the LIBS signals for P and for major and side elements.

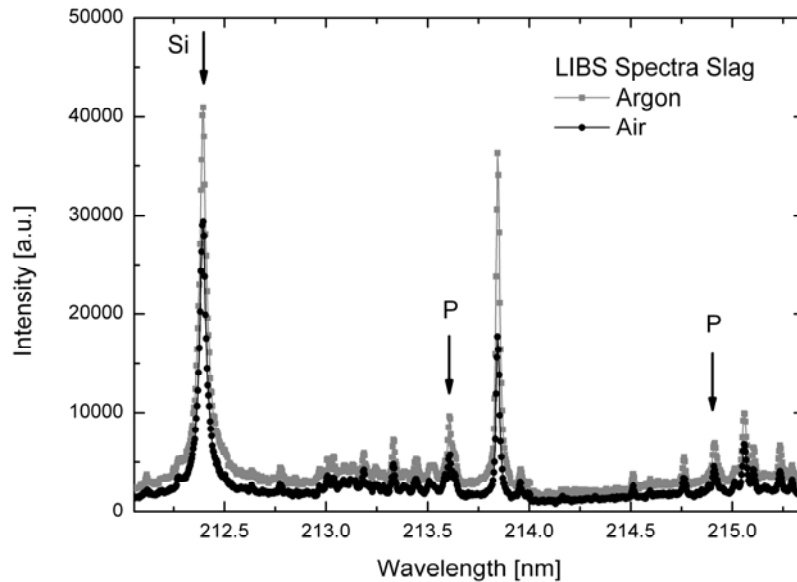


Fig. 2 – Phosphorous signals in the UV range in LIBS spectra from slag samples: Comparison of measurements in argon (grey, squares) and air (black, circles). The two strongest P I lines in the UV spectral region and the strong Si I line at 212.412 nm are marked by arrows.

## 2. EXPERIMENTAL

### 2.1. LASER-INDUCED BREAKDOWN SPECTROSCOPY

Two different experimental LIBS setups were employed for measurements of slag and iron oxide from steel production, respectively, which are described in detail in our previous work [4, 5]. The measurements were either performed in the laboratory or with a mobile system on-site in a steel plant. In both setups, sample material was laser ablated from oxide targets in air or argon by focusing the pulsed radiation of a Nd:YAG laser (wavelength either 523 or 1064 nm, pulse duration  $\tau_L \approx 6$  ns, pulse energy  $E_L \leq 250$  mJ, repetition rate  $f_r \leq 20$  Hz) onto the sample. The laser spot diameter on the target surface was in the order of 1 mm. In most experiments, the samples were rotated during ablation to obtain mean signals representative for samples and to avoid the formation of deep craters. The optical emission of laser-induced plasma was collected by direct coupling to a fiber at oblique angle to the sample (Fig. 1). LIBS spectra were measured with an Echelle spectrometer (LTB, model Aryelle) equipped either with a mechanically gated or an intensified CCD camera. The spectra were recorded for a wavelength range from 190 nm to 360 nm and had a resolution  $\lambda/\Delta\lambda$  of 16,500. For evaluation of the spectra, the peaks were identified with help of the Kurucz Atomic Spectral Line

Database [6] or the NIST Atomic Spectra Database [7] and fitted by Lorentzian line profiles. Measured emission intensities were accumulated at the detector over a number of laser pulses  $N_L$  (*e.g.*, 100 pulses) and the resulting spectrum was normalized to the spectrally integrated total intensity or a spectral line of a reference element of known concentration. Iron oxide ceramics were investigated using a double-pulse Nd:YAG laser (wavelength 532 nm) and an Echelle spectrometer equipped with a mechanically gated CCD camera. Plasma on the ceramic surface was induced by the first laser pulse and re-excited by the second time-delayed laser pulse. Slag pieces or homogenized slag samples were measured with single-pulse Nd:YAG laser (wavelength 1064 nm) irradiation. Often the laser irradiation was performed in an argon stream, which is blown onto the slag target surface by means of a nozzle. The spectra were measured by an Echelle spectrometer equipped with an intensified CCD camera (ICCD). The intensifier allows fast and flexible gating, but also contributes to the background noise, while spectra recorded with the CCD with the mechanical shutter may have better signal-to-noise ratios (for a detailed comparison see [5]).

## 2.2. IRON OXIDE CERAMICS

Iron oxide powder materials are a side product of steel production. They are technologically relevant materials and have received much attention owing to their potential for applications in different fields. One example is the production of soft and hard ferrite components for electronic devices. Especially for this specific application, iron oxide with a high grade of purity is required, including a low content of phosphorous. In this study, the iron oxide material was transformed into ceramic pellet, which allows easier sample handling. The ceramics were produced from iron oxide powder containing ~99 wt%  $\text{Fe}_2\text{O}_3$  and several side and trace elements. Ceramic iron oxide targets with a diameter of 11 mm were produced by sintering of pressed powder pellets at 1000 °C for 12 hours in air. The sintering process resulted in a phase change of the iron oxide in the ceramic to  $\text{Fe}_3\text{O}_4$ .

## 2.3. SLAG FROM STEEL PRODUCTION

Slag from steel production comprises several major and minor oxides such as CaO,  $\text{Al}_2\text{O}_3$ , MgO, Fe-O,  $\text{SiO}_2$ , MnO, etc. The concentration of these oxides and the structure of the material are strongly varying for different types of slag. The fast quantitative analysis of trace elements like phosphorous in such materials is therefore demanding, but the gained information would be important for efficient process and quality control in steel making. Slag pieces were taken from the steel ladle by an automated sampling system and measured either on-site in the steel plant within a few minutes using a mobile LIBS system with single-pulse Nd:YAG

laser (wavelength 1064 nm) or later with the same system in our laboratory. In some cases the slag samples were homogenized by milling and sintering using a similar process as described above.

#### 2.4. PLASMA CHARACTERIZATION

The laser-induced plasma is transient with a typical lifetime of about 50  $\mu\text{s}$  in air and a maximal plasma length in the order of 1 mm. The delay time  $t_d$  after the (second) laser pulse and the gate time  $t_g$  of the CCD detector were optimized for relatively high signal and low background intensities and for small variation of plasma temperature  $T_e$  and electron number density  $N_e$  during the detection time window. Under the assumption of a local thermal equilibrium, the values of  $T_e$  and  $N_e$  can be derived directly from the spectra by means of Saha-Boltzmann plots and the evaluation of the Stark line broadening (*e.g.*, of the H- $\alpha$  line) [8]. Typical values for LIBS measurements of slag materials were  $N_e \approx 10^{17} \text{ cm}^{-3}$  and  $T_e \approx 10,000 \text{ K}$ . The electron temperature and the degree of ionization of the plasma can be increased by re-excitation with the second time-delayed laser pulse in the double-pulse configuration or by the use of argon as background gas, which has a lower breakdown threshold, higher density, and less internal degrees of freedom compared to air. Both methods (*i.e.*, double-pulse and argon) can result in considerably higher line intensity and better signal-to-noise ratios for many emission lines in LIBS. The enhancement by use of argon as a background gas is demonstrated exemplarily in Fig. 2 in LIBS spectra of a slag sample with and without argon flow. Practically all lines in the spectrum in argon show higher line intensities compared to the spectrum in air, including the UV phosphorus lines.

#### 2.5. CALIBRATION CURVES AND STATISTICAL EVALUATION

The evaluation of limits of detection (LODs) is based on calibration curves, where the measured line intensities of LIBS spectra of several samples with different concentrations of the analyte are correlated to reference data measured in the analytical chemical laboratories of voestalpine Stahl GmbH. They were based either on x-ray fluorescence (XRF), spark discharge OES, or wet chemical analysis in combination with inductively coupled mass spectroscopy (ICP MS), depending on the element and the matrix material under investigation. For each sample, the mean value and standard deviations of the LIBS signals were calculated. The data points for samples of different concentrations were fitted by a linear regression by means of the data analysis program package Origin 8.5. If the slope of the regression fit  $b$  has no too high uncertainty, the LOD can be estimated by the formula  $\text{LOD} = 3\sigma/b$ , where  $\sigma$  is the mean standard deviation of the samples with the lowest concentrations. More elaborated techniques as the confidence band method are described, *e.g.*, in [9].

### 3. RESULTS AND DISCUSSION

#### 3.1. IRON OXIDE CERAMICS

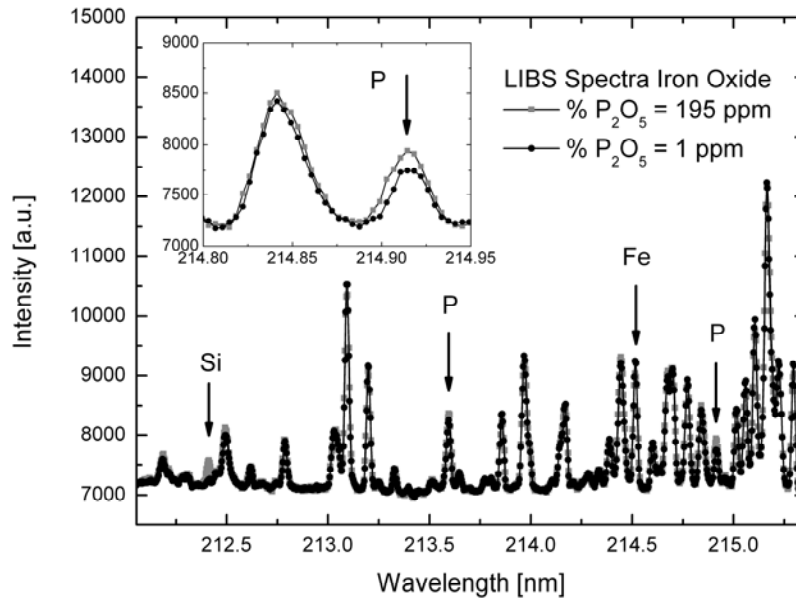


Fig. 3 – LIBS signals in the UV range in spectra from iron oxide ceramic samples: Comparison for two different samples with phosphorous content of 195 ppm  $P_2O_5$  (grey, squares) and 1 ppm  $P_2O_5$  (black, circles). The arrows indicate the same lines as in Fig. 2 and the Fe I line at 214.519 nm. The inset shows a magnification of the spectra near the relevant P I line at 214.915 nm.

Figure 3 shows LIBS spectra of two different iron oxide ceramic samples with a nominal content of 195 ppm and 1 ppm of  $P_2O_3$  referred to weight fractions. These concentration values were obtained from the reference analysis of the powder. The two samples had also different contents of silicon. The other not identified peaks in the spectra originate mostly from iron. It is clear that there is some interference between the phosphorous and iron lines. However as is described in more detail in [5], the use of the double-pulse configuration and of a low-noise CCD detector enabled a clear distinction of both samples regarding their phosphorous content. This is clearly seen in the inset of Fig. 3, which shows an enlarged part of the spectra near the relevant P I line at 214.915 nm. This line is interfered by the weak Fe I line at 214.917 nm. The Fe I lines at 214.840 nm are nearly identical, because no other element line of the constituents of the two different samples appears here.

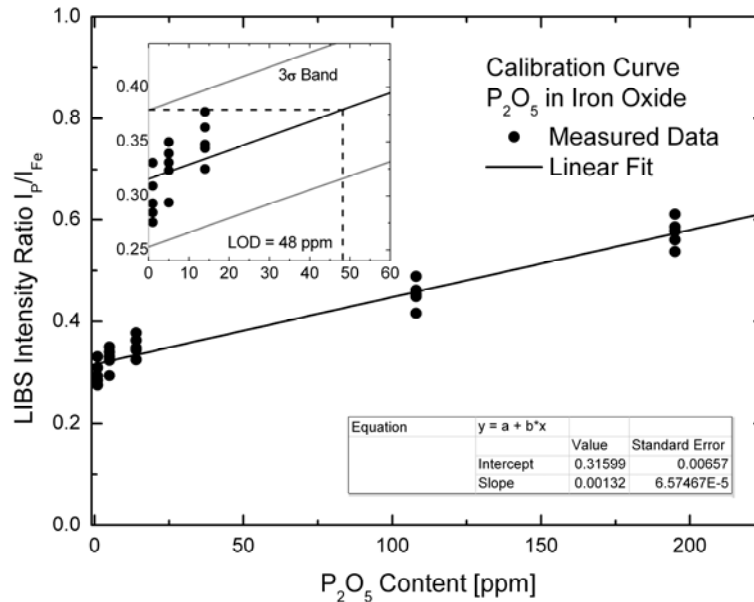


Fig. 4 – Calibration curve of phosphorous content in iron oxide ceramics: LIBS intensity ratio of P I line at 214.915 nm divided by Fe I line at 214.519 nm versus reference analysis. The black line is the linear regression fit (parameters shown in the table). The magnified inset shows results of low concentration samples used for derivation of the  $\sigma$  values.

The intensity of the P I line at 214.915 nm of several iron oxide ceramic samples was used to construct a calibration curve, which is shown in Fig. 4. For compensation of shot-to-shot and sample-to-sample differences of the laser-induced plasma, the intensity of this P I line was normalized to the intensity of the Fe I line at 214.519 nm, which is marked in Fig. 3. Here, we used the assumption that all iron oxide ceramic samples under investigation had practically identical iron oxide content. The LIBS intensity is correlated with the results of reference analysis, which gives the P<sub>2</sub>O<sub>5</sub> content of the Fe<sub>2</sub>O<sub>3</sub> powder used for ceramic production. The relative high intercept value of the regression fit with the axis of 0.31599 is due to the fact, that there is overlap of the P I line at 214.915 nm and the Fe I line at 214.917 nm, as shown in Fig. 3. Nevertheless, the LOD value for phosphorous of 48 ppm is to our knowledge one of the best values achieved by LIBS using the lines in the UV.

### 3.2. SINTERED SLAG POWDER SAMPLES

Figure 5 shows LIBS spectra of two homogeneous sintered slag powder samples of different phosphorous content near the relevant P I line at 214.915 nm. The first sample is made from a certified standard material ECRM 878-1 with a

certified weight fraction of  $P_2O_5$  of 290 ppm. This standard material was purchased from BAM in Berlin, Germany. The second sample is a product sample from the steel work of voestalpine Stahl GmbH (charge number 854011). The phosphorous content obtained by reference analysis of voestalpine Stahl GmbH is  $P_2O_5 = 70$  ppm. The standard material shows a clear P I line at 214.915 nm. This line can be distinguished from the background also for the second sample. Many slag samples have considerable iron oxide contents due to the contact to the liquid steel bath. However, an overlap with an underlying Fe I line at 214.917 nm can be excluded for the spectra in Fig. 5, because otherwise the second Fe I at 214.840 nm should also be visible similar as in the inset of Fig. 3. From this, we estimate that the LOD for  $P_2O_5$  in homogenized slag is around 70 ppm.

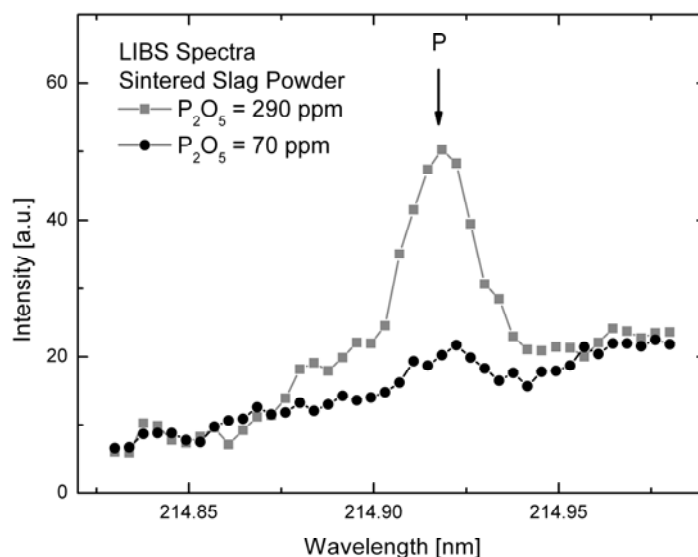


Fig. 5 – LIBS signals in the UV range from sintered slag powder samples: Comparison for two different samples with phosphorous content of 290 ppm  $P_2O_5$  (grey, squares) and 70 ppm  $P_2O_5$  (black, circles). The arrow indicates the P I line at 214.915 nm.

### 3.3. SLAG FROM STEEL PRODUCTION

Figure 6 shows the calibration curve for phosphorous in slag pieces, which were taken from the steel ladle by an automated sampling system directly from the steel making process. The LIBS data are based on LIBS intensities  $I_P$  of the PI line at 214.915 nm and were correlated to reference analysis, which was in this case XRF. For compensation of shot-to-shot and sample-to-sample differences of the laser-induced plasma, the intensity  $I_P$  of this P I line was normalized to the intensity  $I_{Si}$  of the Si I line at 212.412 nm, which is marked in Fig. 2. The slag

samples under investigation here had different contents of the major constituents, including considerable variations of the silicon content. This is taken into account by calculating the LIBS signal for P by  $c_p = I_p/(I_{Si}/c_{Si})$ , where  $c_{Si}$  is the concentration of Si (in wt%). Because  $I_p = \text{const.} \times c_p$  and  $I_{Si} = \text{const.} \times c_{Si}$ , also  $c_p = I_p/(I_{Si}/c_{Si})$  has the unit wt%. The LOD value of  $P_2O_5$  in slag pieces from steel production obtained by the  $3\sigma/b$  method was 0.17 wt%. Without this procedure, the LOD value is higher due to strong scattering of the  $I_p$  data points. The calculation of the LIBS signal of P needs the knowledge of the Si content in the samples, which seems not to be possible in on-site analysis. However, we have demonstrated recently that it is possible to obtain the concentrations of the major constituents of slag including Si directly from the LIBS spectra by a calibration-free approach without using calibration curves and reference samples [4].

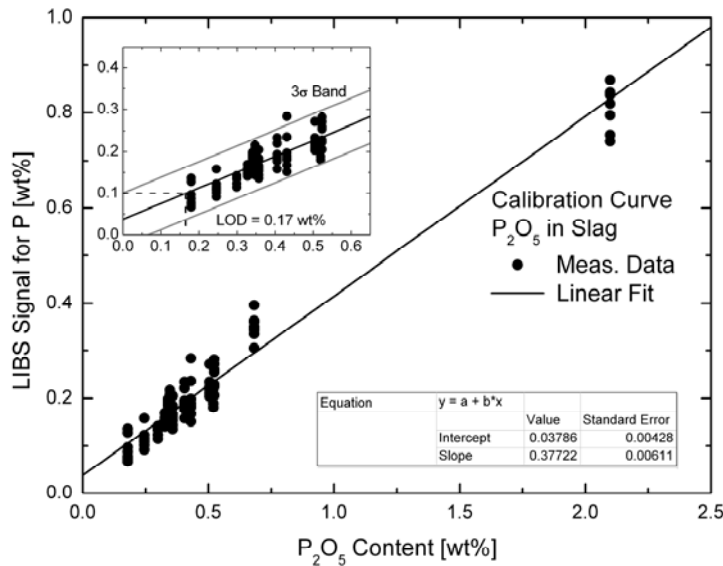


Fig. 6 – Calibration curve of phosphorous content in slag from steel production: LIBS signal for P (*i.e.*,  $c_p = I_p/(I_{Si}/c_{Si})$ ) with P I line at 214.915 nm and Si I line at 212.412 nm versus reference analysis. The black line is the linear regression fit (parameters shown in the table). The magnified inset shows results of low concentration samples used for derivation of the  $\sigma$  values.

The obtained LOD value of Fig. 6 is worse than the values estimated in paragraph 3.2 for homogenized sintered slag samples. We have made LIBS analysis also from drawn slag pieces with lower phosphorous concentrations than in Fig. 6, but did not obtain peaks, which were clearly distinguishable from the background noise. We attribute this result to the fact, that the surface of the drawn sample was less well defined and flat than that of the pressed and sintered samples. Also, the phosphorous may not be distributed homogeneously in the slag and their

may be separation of different phases during solidification of the liquid slag in sample drawing (*i.e.*, there may be less phosphorous at the surface). In reference analysis a larger amount of material is analyzed, which is homogenized by milling and pressing with a binder. However, this processing is time consuming, while the LIBS analysis can provide results within a few minutes after sample drawing and samples can also be analyzed at elevated temperatures of a few hundred degrees Celsius [10].

#### 4. CONCLUSIONS

We have demonstrated that it is possible to analyze the phosphorous content in iron oxide materials and slag materials from steel production by means of LIBS using emission lines in the UV spectral range. The achieved limit of detection obtained with the  $3\sigma/b$  method was in the order of 50 ppm (wt) for  $P_2O_5$  in  $Fe_3O_4$  ceramics and around 70 ppm (wt) for homogeneous sintered slag samples, respectively. For slag pieces drawn directly from the steel ladle, the calculated limit of detection for  $P_2O_5$  was 0.17 wt%. The  $3\sigma/b$  method gives a conservative estimation of the sensitivity, more elaborated techniques as the confidence band method can result in lower values for limits of detection.

**Acknowledgements.** Financial support by the Austrian Federal Ministry of Economy, Family and Youth and the National Foundation for Research, Technology and Development (Christian Doppler Laboratory LAD) is gratefully acknowledged.

#### REFERENCES

1. R. Noll, *Laser-Induced Breakdown Spectroscopy Fundamentals and Applications*, Springer-Verlag, Berlin, Heidelberg, 2011.
2. A.W. Miziolek, V. Palleschi, I. Schechter, *Laser-Induced Breakdown Spectroscopy (LIBS), Fundamentals and Applications*, Cambridge University Press, Cambridge, 2006.
3. D.A. Cremers, L.J. Radziemski, *Handbook of Laser-Induced Breakdown Spectroscopy*, John Wiley & Sons Inc, New York, 2006.
4. J.D. Pedarnig, P. Kolmhofer, N. Huber, B. Praher, J. Heitz, R. Rössler, *Appl. Phys.*, **A 112**, 105–111 (2013).
5. H. Heilbrunner, N. Huber, H. Wolfmeir, E. Arenholz, J.D. Pedarnig, J. Heitz, *Spectrochim. Acta*, **B 74–75**, 51–56 (2012).
6. \*\*\* <http://www.pmp.uni-hannover.de/cgi-bin/ssi/test/kurucz/sekur.html> 2013.
7. \*\*\* <http://www.nist.gov/pml/data/asd.cfm> 2013.
8. B. Praher, R. Rössler, E. Arenholz, J. Heitz, J.D. Pedarnig, *Anal. Bioanal. Chem.*, **400**, 3367–3375 (2011).
9. J.-M. Mermet, *Spectrochim. Acta*, **B 65**, 509–523 (2010)
10. S. Eschlböck-Fuchs, M.J. Haslinger, A. Hinterreiter, P. Kolmhofer, N. Huber, R. Rössler, J. Heitz, J.D. Pedarnig; *Spectrochim. Acta B*, published online 2013. <http://dx.doi.org/10.1016/j.sab.2013.05.023>.